Research Square

Preprints are preliminary reports that have not undergone peer review.
They should not be considered conclusive, used to inform clinical practice,
or referenced by the media as validated information.

Behavior of Concrete One-Way Slab Reinforced by GFRP Bars with a Novel Method of Reinforcement Splices

Omar Z. Amer
University of Anbar
Aleaa B. Radi
University of Anbar
Ziadoon Mohsin Ali
University of Anbar
Akram S. Mahmoud
dr.akramsh1@uoanbar.edu.iq
University of Anbar
Taghreed Kh. Mohammed
Koya University - Kurdistan Region of Iraq
Aymen H. Fayyadh
University of Anbar

Research Article

Keywords: GFRP bars, One-way concrete slab, Reinforcement splice, Flexural behavior, and ACI 440.1

Posted Date: November 26th, 2026

DOI: https://doi.org/10.21203/rs.3.rs-11661402/v1

License: This work is licensed under a Creative Commons Attribution 4.0 International License.
Read Full License

Additional Declarations: No competing interests reported.

Behavior of Concrete One-Way Slab Reinforced by GFRP Bars with a Novel Method of Reinforcement Splices

Omar Z. Amer[1], Aleaa B. Radi[2], Ziadoon Mohsin Ali[3], Akram S. Mahmoud[4]
Taghreed Kh. Mohammed[5], and Aymen H. Fayyadh[4]

[1] *Dams and Water Resources Engineering, Engineering College, University of Anbar, Ramadi, Iraq*
[2]*General Directorate of Education in Anbar - Ministry of Education – Iraq*
[3] *Project and construction department, University of Anbar, Ramadi, Iraq*
[4]*Civil Engineering Department, Engineering College, University of Anbar, Ramadi, Iraq*
[5]*Department of Architecture Engineering, Faculty of Engineering, Koya University, Danielle Mitterrand Boulevard, Koya KOY45, Kurdistan Region – F.R. Iraq*

Author Email's

ale19e1007@uoanbar.edu.iq, Omar.zuair@uoanbar.edu.iq, zaydon88@uoanbar.edu.iq, dr.akramsh1@uoanbar.edu.iq , taghreed.khaleefa@koyauniversity.org, , and Aymen.h.f@uoanbar.edu.iq,

ABSTRACT

Fibre-reinforced polymers (FRP) have become a viable alternative to conventional steel reinforcement in concrete structures exposed to severe environmental conditions, owing to their high corrosion resistance and favorable mechanical properties. This study experimentally investigates the flexural behaviour of one-way concrete slabs reinforced with glass fibre-reinforced polymer (GFRP) bars and evaluates the effectiveness of a novel method for splicing GFRP reinforcement. The experimental program consisted of seven simply supported one-way concrete slabs with dimensions of 1000 × 400 × 70 mm, reinforced with 10 mm-diameter GFRP bars. The specimens were subjected to two-point loading until failure, with different reinforcement splice configurations adopted to investigate their influence on structural performance. The experimental variables included the splice configuration and its effect on the flexural response of the slabs. The measured parameters included cracking load, deflection at cracking and ultimate loads, ultimate load-carrying capacity, stiffness, ductility, toughness, and failure mode. The experimental results were evaluated in terms of the influence of the proposed splice method on the development of flexural strength and overall structural performance. The results were also compared with the predictions and design requirements of the ACI 440. Particular attention was given to the serviceability and ultimate limit states, considering the relatively low elastic modulus and different failure characteristics of GFRP reinforcement compared with conventional steel reinforcement. The findings demonstrate the effectiveness of the proposed splice technique and provide insight into its ability to develop adequate structural performance in GFRP-reinforced concrete slabs. The study indicates that an appropriately designed new splice can provide a practical solution for reinforcement continuity while maintaining satisfactory flexural strength, stiffness, and serviceability. The outcomes contribute to the development of more reliable design and detailing practices for GFRP-reinforced one-way concrete slabs, particularly where conventional steel reinforcement is unsuitable because of severe environmental exposure.

Keywords: *GFRP bars, One-way concrete slab, Reinforcement splice, Flexural behavior, and ACI 440.1*

1. INTRODUCTION

FRP reinforcing appeared as a practical resolve, in addition to its non-corrosive characteristics, also due to its high strength-to-weight ratio, and it has good fatigue resistance. The reinforced concrete cracks in tension, but the FRP reinforcement controls or prevents the opening crack and crack width control [1]. The steel reinforcement corrosion is a primary factor contributing to the decline of reinforced concrete structures. The reinforcement with glass fiber-reinforced polymer (GFRP) is a better alternative to the reinforcement of steel and takes a higher ratio of strength to weight due to its brittle behavior and low elasticity value [2]. The property of the bond between reinforcing bars in the concrete is important because it greatly influences the performance of the structural member concerning deformability of concrete, internal damping, as well as instability. The bond interface mustn't deteriorate; Therefore, thus ensuring a sufficient degree of structure strength and ductility. Although a lot of research has been done on the bond properties of steel bars in concrete extensively; for GFRP bars, such information is lacking. Because steel and GFRP bars have differing mechanical and physical properties, it is not possible to assume that they will respond similarly [3]. Members under flexure are affected by strong ductility due to the elastic behaviors of the FRP rebars and the bond properties of FRPs such as the beams and slabs [4]. In comparison to conventional slabs, the response of load deflection for GFRP-reinforced slabs shows a greater decrease in stiffness. where a conventional slab observes a larger increase in deflection through a little change in the load due to the reinforcement yielding, while the reinforced slabs with GFRP show no reinforcement yielding, because of it is low modulus of elasticity while the deflection increases as the load increases [5]. The reinforced slabs with GFRP behaved in a bilinear elastic manner up to failure as well and the increase in the ratio of reinforcement led to less deflection for all tested slabs A high ductility degree, measured by deformability factors in the GFRP-reinforced slabs, was reached in the tested slabs, including all values were greater than 4 [6]. the glass fibers are highly corrosion-resistant by acids, the wrong types of combination of glass fibers with resins may lead to GFRP bars premature deterioration in an alkaline environment. Nevertheless, a lot of buildings made using these bars have been operational in highly competitive environments [7]. The GFRP-reinforced slabs showed bilinear elastic behavior until failure. Compared to the steel-reinforced slabs, their stiffness was considerably reduced after the cracks started, and the strains and deflections were larger than slabs of steel reinforced because of the low elasticity modulus (E_{GFRP} / E_{Steel} ≈ 0.22-0.25) and the characteristics of different bonding of GFRP reinforcement [8]. when replaced (20%) of steel by GFRP reinforcement, there was an (11.3%) increase in toughness because of the increase in the deflection and the load capacity and when the replacement was 40%, the decrease in toughness was 34.7% because of the ductility and the reduction in deflection [9]. There are several types of commercial glass fiber available for some applications, such as Chemical Stable (C), High Strength (S), Electrical grade (E), and Alkali-Resistance (AR) (13). Many researchers and investigators focus on reinforcing the structures with FRP bars including GFRP. They have shown notable enhancement in the behavior of FRP-RC structures rather than conventional plain concrete ([10], [11], [12], [13]).

2. RESEARCH SIGNIFICANCE

An experimental program was carried out in this research work to study; the flexural behavior of concrete one-way slabs reinforced with GFRP bars has to be studied, also tested the slabs under

static load conditions. In addition investigate IFS (Initial flexural stiffness) at the ultimate stage and measured the deflections at cracking load, ultimate load-carrying capacity, ductility, toughness, and stiffness.

3. EXPERIMENTAL PROGRAM

The experimental investigation was conducted on seven simply supported concrete one-way slabs (1000 × 400 × 70 mm) with a cover of (20mm) and reinforced with GFRP bars with different reinforcement splices subject to two-point loading increased gradually every 2kN until failure. **Fig. 1** shows the dimensions and reinforcement details of tested specimens. Three linear variable differential transducers (LVDTs) to evaluate the slab deflection and strain gauges on the GFRP rebar surface to record the strain through the tests. Investigating the structural behaviors of the slabs with various splices of reinforcement of GFRP. Serviceability behavior may be more important than ultimate strength in GFRP-RC slabs Therefore deflections at cracking load, ultimate load-carrying capacity, ductility, toughness, and stiffness were measured in all the models experimentally.

4. MATERIAL PROPERTIES

4.1 Concrete

Table.1 gives the concrete proportions constituents. The ordinary Portland cement was used in the concrete mixture. The compression strength of concrete of a standard (150mm) cube at (7 days). The mix design was done according to the supplied material. the materials (gravel and sand) must be saturated and surface dry condition. The average compression concrete is 49 Mpa and the modulus of elasticity (32900 MPa) for normal-weight concrete is calculated according to (ACI-318) cod [14].

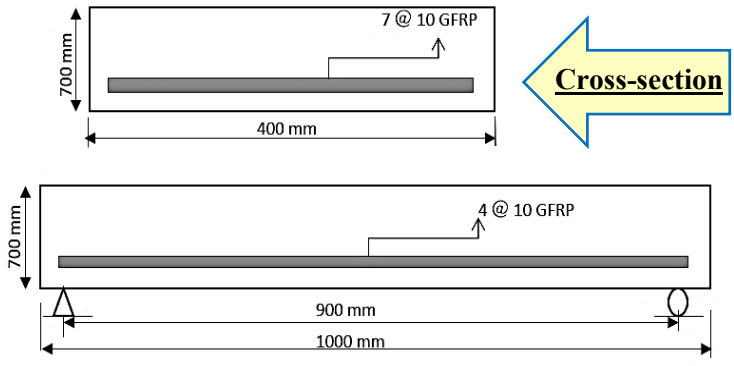

Figure.1 One-way tested slab details

Table.1 The proportions of a concrete mixture

Constituent	Quantity (Kg/m³)
Grave	1060
Sand	710
Cement	500
Water	120
Admixture (Visco Crete 225 S)	5
Actual concrete density	2395

4.2 GFRP bar

The GFRP bars with a nominal diameter of (10mm) and a modulus of elasticity (45 GPa) were used to reinforce the slab. Seven GFRP bars in the long direction of the concrete slab with a length of (980mm) and four bars of GFRP in the short direction with a length of (360mm).

4.3 Slab specimens

The tested slabs are denoted as follows: G1: slab without splice (a continuous bar) four GFRP bars with a length of (98cm) in the short direction of the slab, G2: six GFRP bars (two without splice have a length of (98cm), and four with a length of (64cm) have spliced in the center of a slab with (30cm)), G3: six GFRP bars (two without splice have a length of (98cm), and two with a length of (79cm) have splices in (30cm) with two that are (49cm) long in opposite to one another from a way of the slab center), G4: similar to G2 with the splice region strengthening by the Carbon Fiber Reinforced Polymer (CFRP) sheets, G5: eight GFRP bars with a length of (64cm) have spliced in the center with (30cm) with strengthening by (CFRP), G6: four GFRP bars (two without splice have a length of (98cm), and two with a length of (98cm) cut at an angle of 45 at their ends at a distance of 30, interconnected, one complementing the other and strengthening by (CFRP)), G7: four GFRP bars with a length of (98cm) cut at an angle of 45 at their ends at a distance of 30, interconnected, one complementing the other and strengthening by (CFRP). All models are shown in **Fig. 2.**

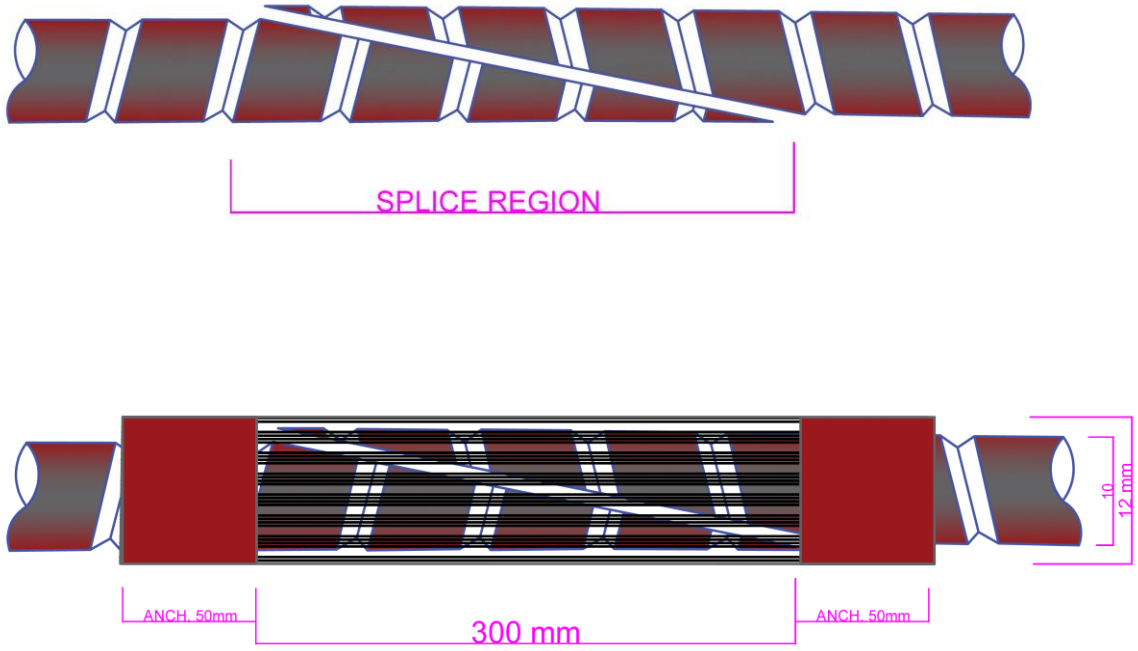

G1	**slab without splice**, four continuous bar GFRP bars with a length of (98cm) in the short direction of the slab	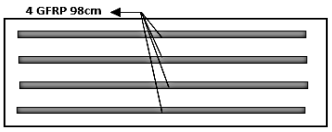
G2	**Center spliced 50% reinforcement**, six GFRP bars (two without splice have a length of (98cm),	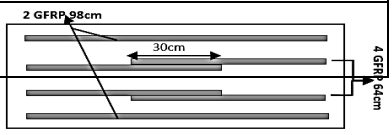

	and four with a length of (64cm) have spliced in the center of a slab with (30cm))	
G3	**Staggered spliced 50% reinforcement**, six GFRP bars (two without splice have a length of (98cm), and two with a length of (79cm) have splices in (30cm) with two that are (49cm) long in opposite to one another from a way of the slab center),	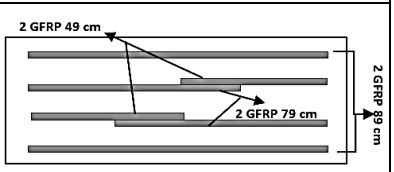
G4	**Strengthened spliced 50% reinforcement**, similar to G2 with the splice region strengthening by the Carbon Fiber Reinforced Polymer (CFRP) sheets,	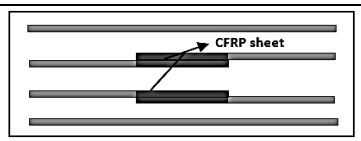
G5	**Strengthened spliced 100% reinforcement,** eight GFRP bars with a length of (64cm) have spliced in the center with (30cm) with strengthening by (CFRP),	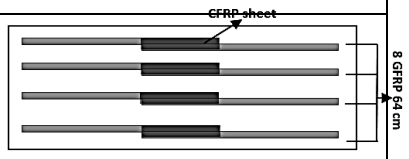
G6	**Strengthened a new spliced 50% reinforcement,** four GFRP bars (two without splice have a length of (98cm), and two with a length of (98cm) cut at an inclined angle at their ends at a distance of 30, interconnected, one complementing the other and strengthening by (CFRP)),	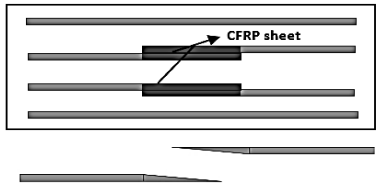
G7	**Strengthened a new spliced 100% reinforcement,** four GFRP bars with a length of (98cm) cut at an inclined angle at their ends at a distance of 30, interconnected, one complementing the other and strengthening by (CFRP).	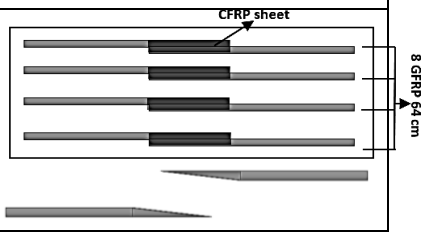

5. TEST RESULTS AND DISCUSSIONS

The results of the experiment are presented. The slabs were instrumented with three LVDTs (one on the left, one on the right, and one on the middle) and a strain gauge on the splice place of the GFRP rebar during the tests. All the slabs were designed to be subjected to load, with increased applied load, the cracks increased to failure when crushing concrete by degradation in stiffness of the slabs and an increase in the deflection in the center of the slab. In all the tested slabs, the crack appeared directly under the load points and propagated toward the compression face deflections at cracking, and the ultimate load is studied by examining the strain profile of the GFRP reinforcement along the slab. Figures 5, 6, and 7 show the load vs. deflection behavior for all the GFRP-reinforced concrete slabs on the slab's right, mid-span, and left, respectively. The load-strain responses for each GFRP bar are illustrated in Fig. 8. Table 2 summarizes the deflections at cracking load and ultimate load-carrying capacity. While the IFS (Initial flexural stiffness) at the ultimate stage, ductility, toughness, and stiffness are illustrated in Table 3.

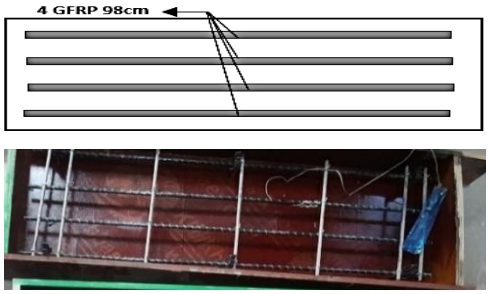

(a) G1 Model

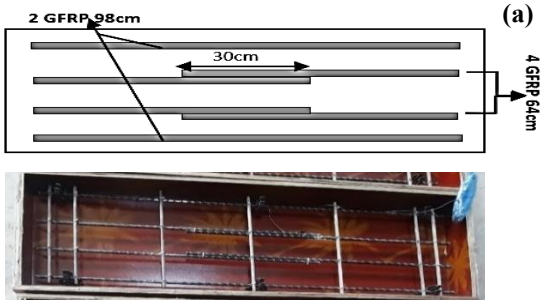

(b) G2 Model

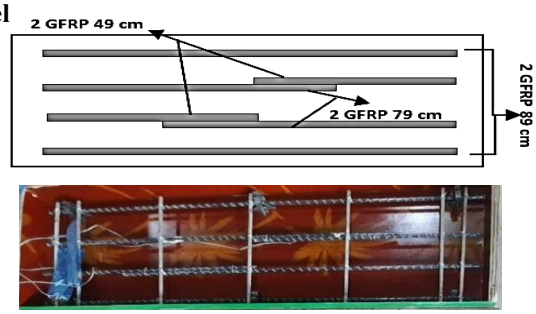

(c) G3 Model

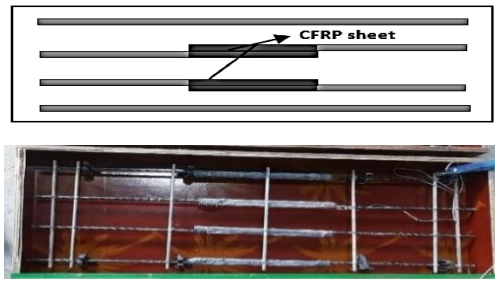

(d) G4 Model

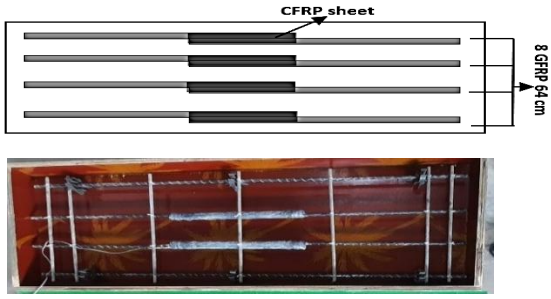

(e) G5 Model

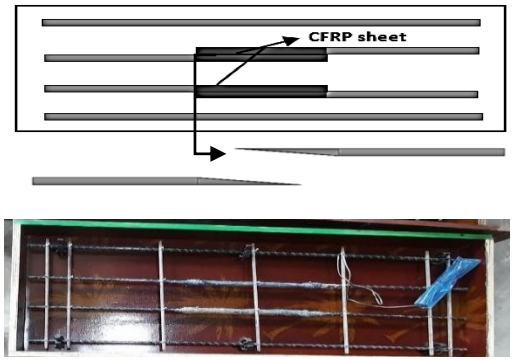

(f) G6 Model

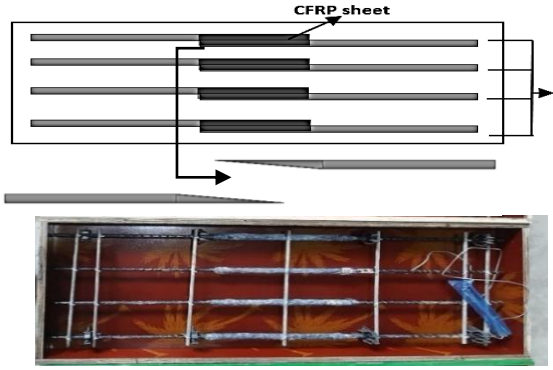

(g) G7 Model

Figure.2 (a to g) Laboratory image and diagram of models

Table.2 Deflections at the crack, and ultimate loads for GFRP-RC slabs

No.	Slab	P_{cr}	$\triangle_{cr}$	P_u	$\triangle_u$
1	G1	5.5	1.21	35.3	41.8
2	G2	8	0.31	42.62	26.68
3	G3	7.5	0.40	46.62	34.78
4	G4	6	0.32	35.3	26.01
5	G5	7.5	0.38	40.63	21.91
6	G6	6.5	0.31	39.69	29.7
7	G7	5.5	0.53	39.29	29.28

Table.3 Initial flexural stiffness, Ductility, Toughness, and stiffness

No.	Slab	IFS (kN/mm) ($P_{cr}/\triangle_{cr}$)	IFS at ultimate stage (kN/mm) ($P_u/\triangle_u$)	Ductility	Toughness (kN.mm)
1	G1	4.55	0.84	1.52	905.18
2	G2	25.81	1.60	3.22	804.27
3	G3	18.75	1.34	2.58	1094.5
4	G4	18.75	1.36	3.59	893.56
5	G5	19.74	1.85	2.36	596.56
6	G6	20.97	1.34	3.02	872.12
7	G7	10.38	1.34	1.86	810.72

6. CRACK PATTERN OF TESTED SPECIMENS

Fig. 3 shows the crack patterns in the slabs with different splices. At first, all the slabs were uncracked. However, as the load increased, some cracks started to appear. More cracks then developed along the slabs as the load increased. All the samples behaved linearly until cracking, due to the low plasticity in the reinforcement. Cracks appear at the bottom surface of the concrete slab. Flexural failure type occurs in all the slabs at mid-span between two concentrated loads at the applied load of (5.5, 8, 7.5, 6, 7.5, 6.5, and 5.5 kN) for slabs G1, G2, G3, G4, G5, G6, and G7, respectively. The crack propagation in slabs G1, G2, G3, G4, G6, and G7 were similar as the loads increased as shown in **Fig. 3**. Also, **Table.2** shows the cracking loads (P_{cr}). The splicing in GFRP bars increased the crack load with decreased deflection, it was observed that the G2 slab was substantially more effective than the G1 slab (without splice). At a low load of (5.5 kN) immediately after the first cracks, the cracks in specimens (G1 and G7 slab). At a medium load of (6, and 6.5 kN), appeared vertical flexural cracks, where the cracks were higher than at the level of the low load for specimens (G4 and G6 slab). At the stage of high load (7.5 and 8kN), the cracks were deeper than previously for specimens (G3, G5, and G2 slab). The flexural cracks that develop in the flexure span in every crack correspond to a drop in the load-deflection curve [15]. **Load–deflection**

The tested slabs were classified into multiple models according to their bond as shown in **Fig.2**. The load-deflection curves of the tested slabs at mid-span are shown in **Fig. 5**. All slabs show an initial linear behavior that ends with the first concrete crack. The first change in the response of the load-deflection slope curve corresponds to the specimen's flexural cracking. Larger deformations are obtained for slabs whose bars do not contain a connection, and vice versa, the more the number of connected bars and the more reinforced they are, the less the deflection. The slab G3 shows a larger ultimate load, more than other models. Where the G1 and G4 show

a lower ultimate load, the G1 and G4 slab deflections were 41.8 mm and 26.01 mm, respectively, at 35.3 kN. This is due to the splice of the GFRP bars in the G4 model and their strengthening with the CFRP sheet in the middle. This resulted in a deflection of the G1 model twice that of the G4 model as shown in **Table.2**. The Slab G6 model reached a deflection of 29.7 mm at an applied load of 39 kN, whereas its corresponding slab G7 model reached a deflection of 29.28 mm under the same load. Although the two models have a 45-degree cutting bar attached to the middle rod and are strengthened with a CFRP sheet, the G7 model has spliced and strengthened eight rods instead of four bars. The right and left deflection values were relatively close, indicating symmetrical slabs bending as shown in **Fig.6 (a), and (b)**.

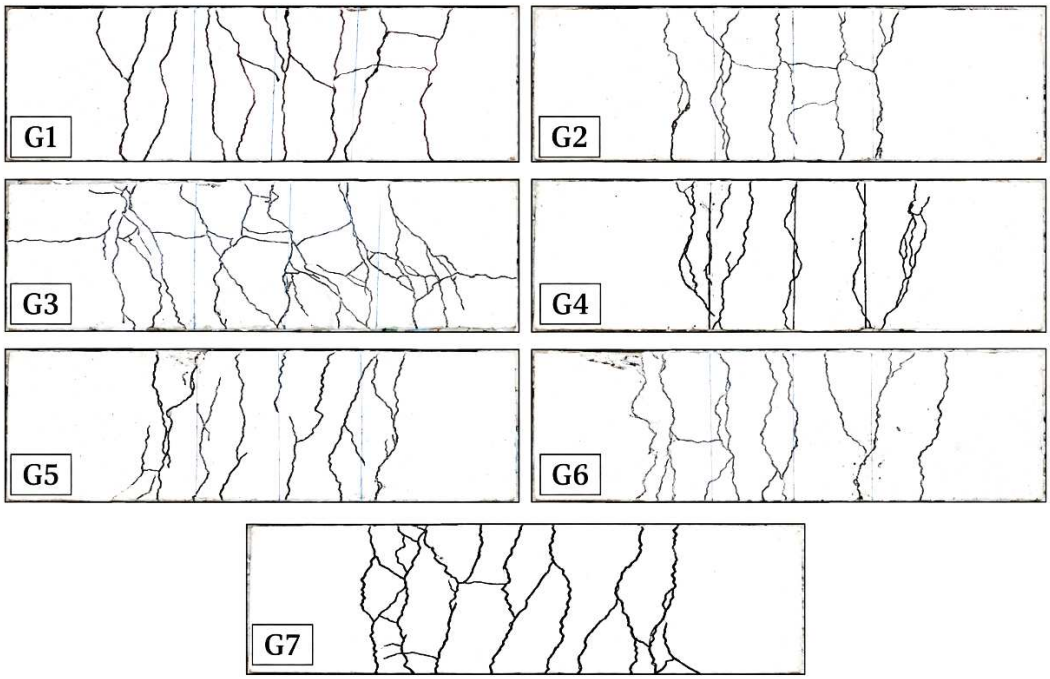

Figure.3 Crack patterns at the failure of the tested slab.

7. FLEXURAL STIFFNESS

The stiffness degree at large deflection is one characteristic that makes the GFRP-RC unique [16]. The stiffness of the slabs is known from the load-deflection curve response, as seen in **Fig.5** the increase in the amount of several slices wrapped with CFRP sheets increased the flexural stiffness in the post-cracking stage. **Fig. 5** shows that the GFRP-RC slab without a splice (G1 model) shows a larger reduction in stiffness than the slab with a splice. The global stiffness for the G1 slab model was significantly lower than the other models. At the crack stage, the stiffness in the G2 model was increased by 467.25% from the G1 model, by 312% in the two models G3 and G4, and by 333.84%, 360.87%, and 128% in G5, G6, and G7, respectively. After cracking started at the ultimate stage, the increase in stiffness was as follows: by (90.43, 59.5, 61.6, 120.2, 59.5, and 110.7%) in G2, G3, G4, G5, G6, and G7 respectively the reason is due to the number and method of splicing the bars and the presence of strengthening in the connecting area and also depending on the method of connection Whereas the G5 model and the G7 model contain 8 bars of GFRP splice in the middle and wrapped in CFRP, this makes

the stiffness have more improving than the other of the models. Also, the amount of reinforcement significantly affects the deflection and thus affects the stiffness of the slab. The crack's flexural stiffness was lower, and there was greater deflection. The load-deflection curves clearly show this finding.

8. DUCTILITY AND TOUGHNESS

Ductility is defined as the inelastic energy dissipation in the structure that enables the redistribution of the internal forces when the structure is close to failure. The ductility is based on deflections, which calculate the ultimate deformation-to-yield deformation ratio. The ductility of GFRP-reinforced concrete cannot be described by this concept since the GFRP-reinforced members show no yield behavior [17]. Because of the GFRP bar's linear behavior, many approaches are used to evaluate the GFRP-reinforced member's ductility including an energy-based method [18] and calculated by Eq (1):

$$\mu_E = 0.5\left(\frac{E_t}{E_e} + 1\right) \qquad \ldots\ldots (1)$$

Where μ_E is the ductility index, E_t is the total energy finding as the area under the curve of load-deflection, E_e the elastic energy finding as the hatch area in **Fig. 4,** and calculated as:

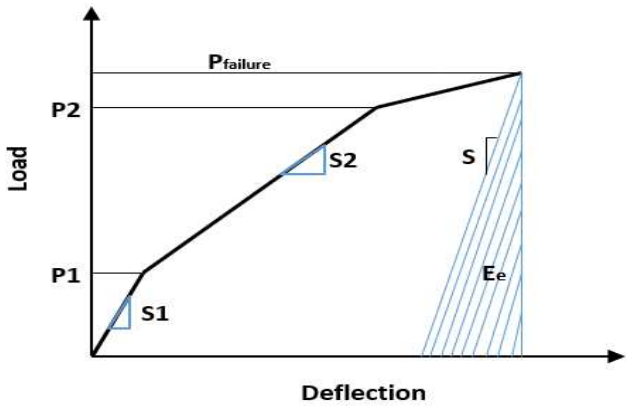

Figure.4 Energy-based model as suggested by (19).

$E_e = \frac{{P_u}^2}{2S}$ ...(2), where S is calculated as (2):

$$S = \frac{P_1 S_1 + (P_2 - P_1) S_2}{P_2} \qquad \ldots(3)$$

P1 is the cracking load (P_{cr}), and P2 is the load that the specimen's stiffness changed before failure. P2 is almost equivalent to the ultimate load (P_u) [10]. Ductility must be designed for the whole system to avoid sudden brittle failure. The ductility indexes of the G4 and G6 models were approximately (200%) and (175%), respectively, higher than the ductility index of the G1 model. The inclusion of splices of bars and adding wrapped with CFRP sheet can likely overcome and improve the low ductility of GFRP bar-reinforced slab. the ductility decreases with increased reinforcement as in the G5 and G7 models. Toughness is also known as the total absorbed energy. It is determined by computing the load-deflection curves of the slabs The absorbed energy is calculated as the area under the (load-deflection) curve[19-22]. The results

in **Table.3** indicates that the modified splice has good durability When compared to the G1 specimen.

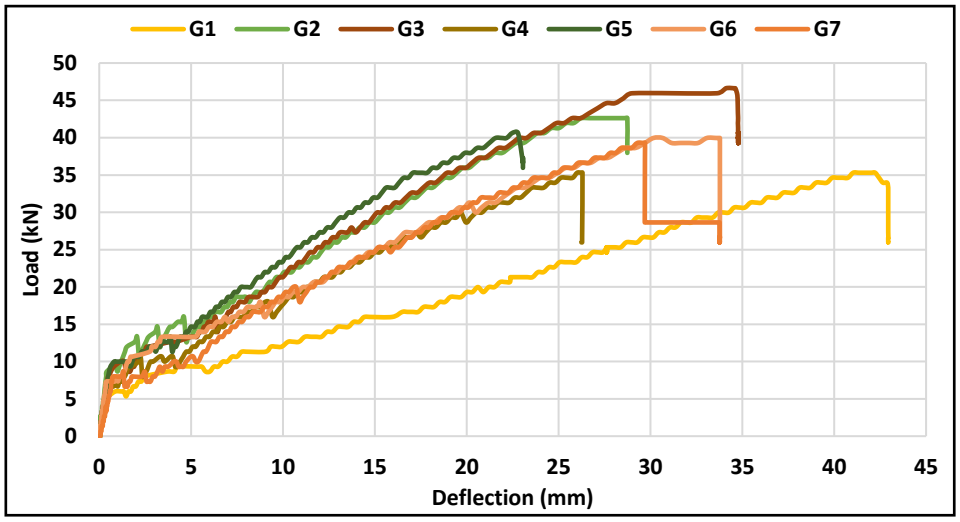

Figure.5 Load-deflection for mid-span slabs of models (G1, G2, G3, G4, G5, G6, and G7)

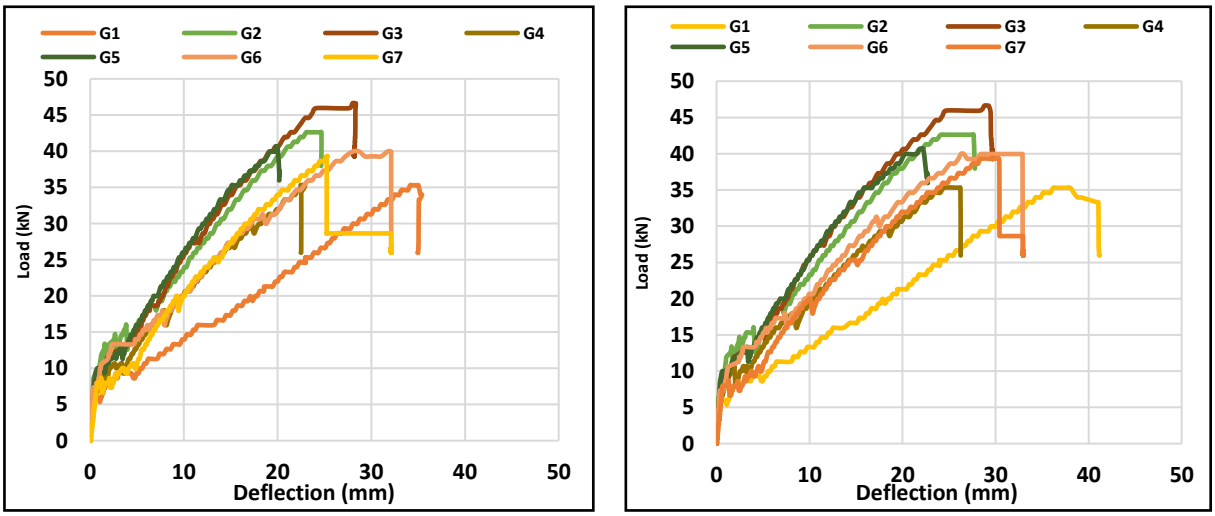

(a) (b)

Figure.6 Load-deflection for the (G1, G2, G3, G4, G5, G6, and G7 models) at (a) the left side, and (b) at the right side.

9. STRAIN IN THE GFRP BAR

For the same splice of bars, the deformations are affected by the strengthening splice area. The GFRP-RC slab rods showed a bi-linear load-strain relationship as shown in **Fig.8**. The strains at the same ultimate load recorded in slab strips G6 and G7 were 33.57 and 29.28 με, respectively, so the use of CFRP sheet enhanced the characteristics of the bond of the GFRP bars in concrete. The experimental observations indicate that reinforcement splice detailing plays an important role in the flexural response of GFRP-reinforced concrete slabs. Differences in the load–strain curves reflect variations in the development of cracking and the subsequent stresses within the tested specimens. However, the assessment of deformation capacity and energy absorption requires additional consideration of the complete load–deflection relationships and the corresponding ductility and toughness indices. Although the specimens

generally exhibited progressive load development, noticeable differences were observed in the initial loading stage, the transition following cracking, and the subsequent increase in load. These differences suggest that the reinforcement splice configuration influenced how stresses were transferred between the GFRP bars and the surrounding concrete, particularly after the formation of the first cracks. However, in this section, the referenced specimens (Figure 8 a-c) show the regular result, addressing the G3 with splices having less strain vs the load limit because less redistribution in internal forces for un-strengthened specimens.

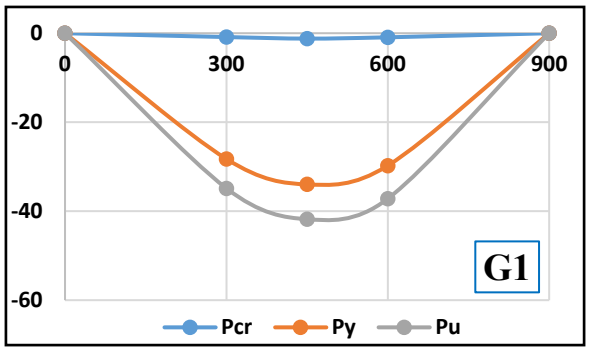

(a)

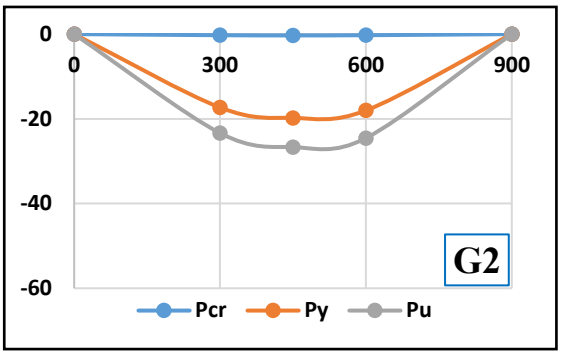

(b)

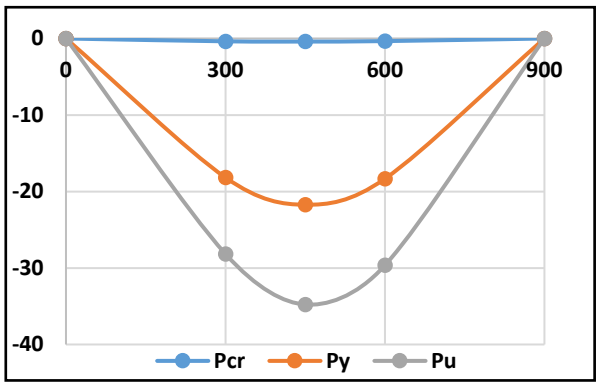

(b)

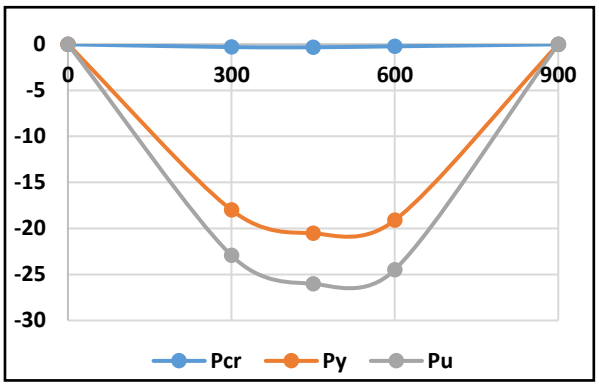

(d)

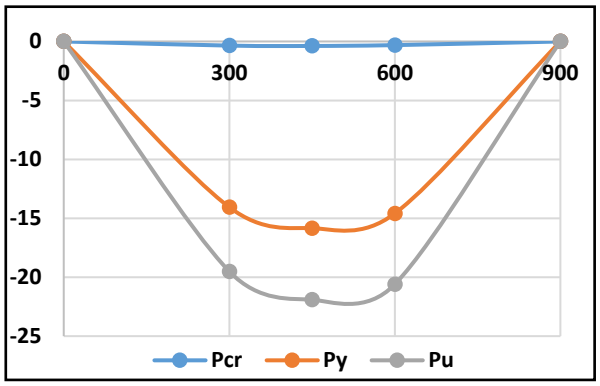

(e)

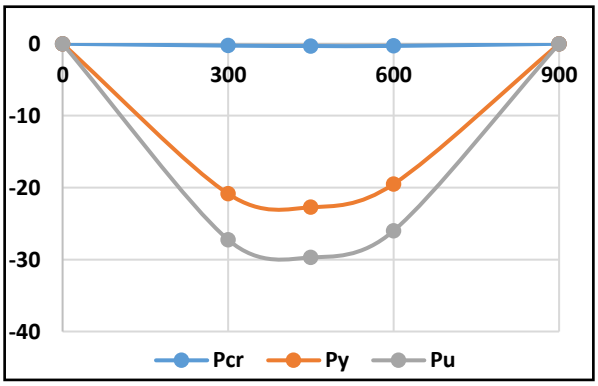

(f)

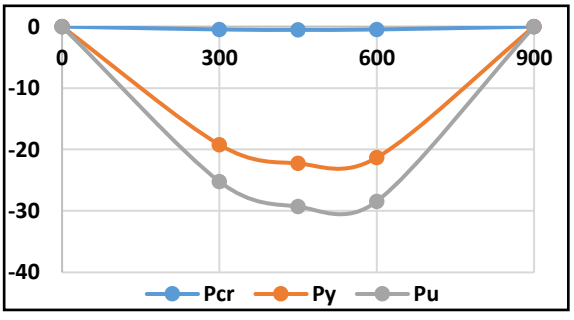

(g)

Figure.7 Deflection profile of slabs (a) G1, (b) G2, (c) G3, (d) G4, (e) G5, (f) G6, and (g) G7 models

For specimen G4 (Figure 8d), the load initially decreased slightly from approximately 11 to 9 kN before beginning to increase progressively with increasing strain. This change in response may be associated with the formation of initial cracks and the subsequent redistribution of stresses within the slab. Beyond this stage, the specimen exhibited a relatively continuous increase in load, reaching approximately 33–34 kN at a strain of about 30×10^{-3}. The corresponding experimental results in Table 2 indicate a cracking load of 6.0 kN and an ultimate load of 35.30 kN. The observed behaviour suggests that the specimen was able to develop additional resistance after cracking, although its ultimate capacity remained comparable to that of the control specimen. A different response was observed for G5 (Figure 8e), which exhibited a more extended loading process. Following the initial loading stage, the load increased progressively, with some fluctuations along the curve. Such variations are commonly associated with successive crack development and changes in the interaction between the reinforcement and surrounding concrete. The load eventually approached approximately 40 kN, followed by a relatively stable response. As indicated in Table 2, G5 reached a cracking load of 7.5 kN and an ultimate load of 40.63 kN. These values represent improvements of 36.36% and 15.10%, respectively, compared with the control specimen. The combination of higher cracking resistance and ultimate capacity suggests that this reinforcement arrangement provided a favorable response during both the initial and post-cracking stages. The load–strain relationship of G6 (Figure 8f) was characterized by a relatively stable initial response, followed by a gradual increase in load as the strain developed. The initial portion of the curve indicates that the specimen sustained increasing deformation with relatively limited changes in load before entering a more pronounced loading stage. According to Table 2, the cracking and ultimate loads were 6.5 and 39.69 kN, respectively, corresponding to improvements of 18.18% and 12.44% over the control specimen. This indicates that, despite the relatively moderate improvement in cracking resistance, the specimen maintained a higher ultimate load-carrying capacity. Therefore, the influence of the splice arrangement appears to be more evident in the post-cracking response than in the initial cracking stage. For G7 (Figure 8g), the load initially increased with relatively limited variation, followed by a more noticeable increase after approximately 8×10^{-3} strain. The curve subsequently approached a relatively stable loading stage. Interestingly, although G7 exhibited the same cracking load as the control specimen (5.5 kN), its ultimate load reached 39.29 kN, representing an 11.30% increase. This difference suggests that the adopted reinforcement arrangement had a more pronounced influence on the development of resistance after cracking than on the initial cracking load.

10. CONCLUSIONS

This study experimentally investigated the flexural behaviour of seven GFRP-reinforced concrete one-way slabs incorporating different reinforcement splice configurations. The experimental program focused on evaluating the influence of splice detailing on cracking behaviour, load-carrying capacity, stiffness, ductility, and energy absorption. Based on the obtained results, the following outcomes can be drawn:

1. The experimental results demonstrated that the reinforcement splice configuration had a noticeable influence on the overall flexural behaviour of the GFRP-reinforced concrete slabs. Compared with the control specimen (G1), five of the six investigated

configurations achieved higher ultimate loads, with improvements ranging from 11.30% to 32.07%. Among the tested specimens, G3 exhibited the highest load-carrying capacity of 46.62 kN, representing a 32.07% increase over the control slab.

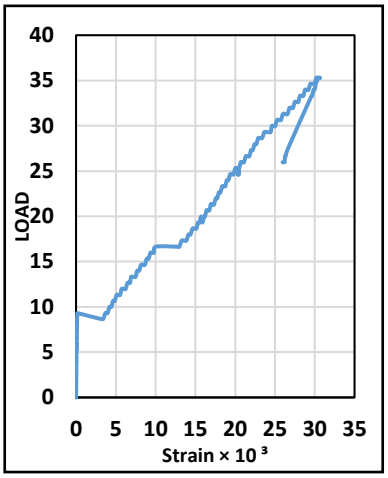

(a)

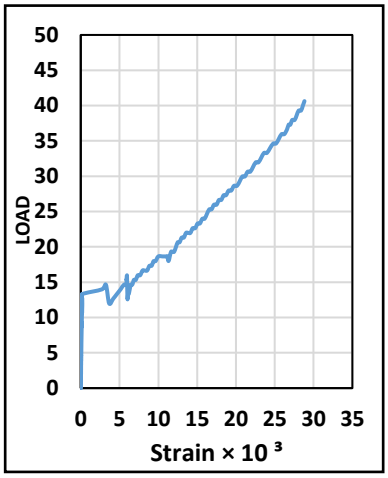

(b)

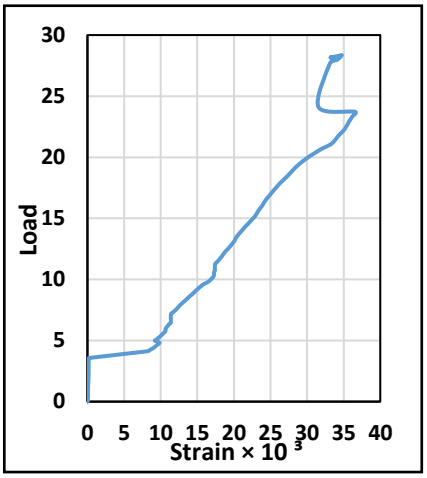

(c)

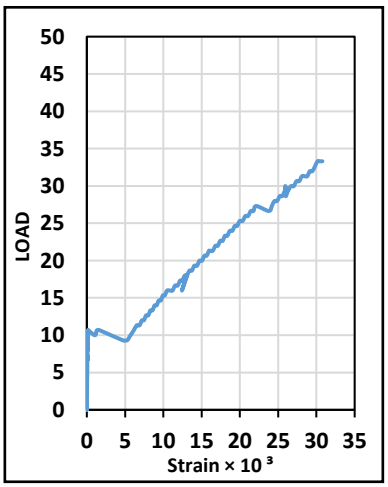

(d)

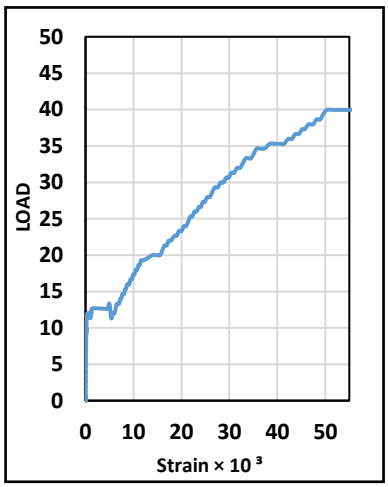

(e)

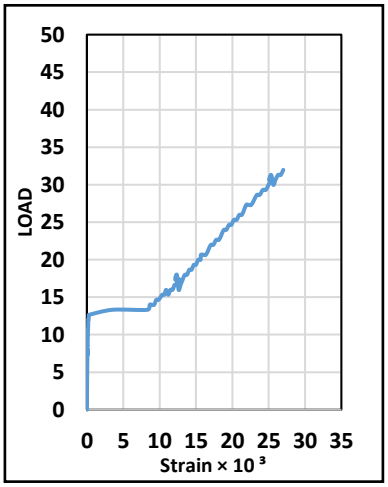

(f)

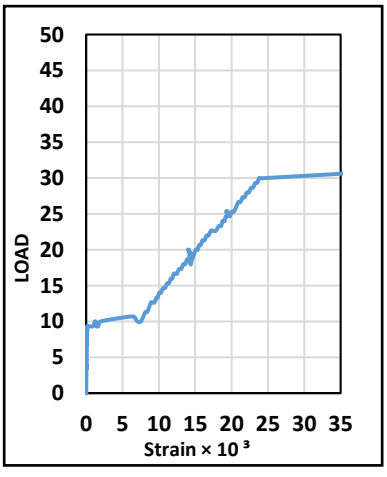

(g)

Figure. 8 Load-strain for a: G1 model, b: G2 model, c: G3 model, d: G4 model, e: G5 model, f: G6 model, g: G7 model.

2. A considerable increase in initial flexural stiffness was observed in all modified specimens relative to the control slab. G2 achieved the highest initial stiffness of 25.81 kN/mm, which was approximately 4.67 times that of G1. This improvement is particularly relevant to the serviceability performance of GFRP-reinforced members, where controlling deformation and cracking is an important design consideration.

3. The stiffness evaluated at the ultimate loading stage followed a different trend from the initial stiffness. G5 recorded the highest value of 1.85 kN/mm, representing an improvement of 120.24% over the control specimen. This difference indicates that the effectiveness of a splice configuration in controlling deformation may vary throughout the loading process and should therefore be evaluated at different stages of structural response.

4. All strengthened spliced-specimens exhibited higher ductility indices than the control slab. The greatest improvement was observed in G4, which achieved a ductility index of 3.59, approximately 136.18% higher than that of G1. G2 and G6 also demonstrated substantial increases of 111.84% and 98.68%, respectively. These results highlight the influence of reinforcement splice detailing on the deformation characteristics of GFRP-reinforced concrete slabs.

5. The toughness results revealed that improvements in strength and stiffness did not necessarily translate into greater energy absorption. G3 achieved the highest toughness of 1094.50 kN·mm, exceeding the control specimen by 20.92%. In contrast, G5 recorded the lowest toughness of 596.56 kN·mm, representing a reduction of 34.09%. This difference emphasizes the importance of considering the complete load–deflection response when evaluating the energy absorption capacity of GFRP-reinforced members.

6. Staggered spliced-specimens provided the most favorable combination of strength and energy absorption, achieving the highest ultimate load and toughness, together with substantial improvements in cracking resistance and initial stiffness. Nevertheless, the results of G2, G4, and G5 demonstrate that the optimum splice configuration depends on the performance parameter being considered. G2 was more effective in improving cracking resistance and initial stiffness, G4 provided the highest ductility, while G5 exhibited the highest ultimate-stage stiffness.

Authors' Contributions

Akram S. Mahmoud contributed to the conceptualization, methodology, supervision, and critical revision of the manuscript. Omar Z. Amer & Ziadoon Mohsin Ali contributed to the experimental investigation, and data collection, Aleaa B. Radi contributed to analysis, and preparation of the initial manuscript draft. All authors contributed to the interpretation of the experimental results, reviewed the manuscript, and approved the final version for publication.

Funding

The authors received no financial support for the research, authorship, or publication of this article.

Data Availability

The datasets generated and/or analyzed during the current study are available from the corresponding author upon reasonable request.

Code Availability

Not applicable.

Declarations

Ethics Approval and Consent to Participate
Not applicable.

Consent for Publication
Not applicable.

Competing Interests
The authors declare that they have no competing interests.

***Clinical Trial Registration*:**
Not Applicable

REFRENCES

[1] *FRP reinforcement in RC structures*. International Federation for Structural Concrete, 2007.

[2] Y. Zheng, C. Li, and G. Yu, "Investigation of structural behaviours of laterally restrained GFRP reinforced concrete slabs," *Compos B Eng*, vol. 43, no. 3, pp. 1586–1597, Apr. 2012, doi: 10.1016/j.compositesb.2011.11.012.

[3] M. Pecce and R. Realfonzo, "Bond between Glass Fiber Reinforced Plastic Reinforcing Bars and Concrete-Experimental Analysis," 2016. [Online]. Available: https://www.researchgate.net/publication/262260072

[4] S. Baliram, G. Nithisha, S. Ganesh, Y. Divya, M. Praneeth Kumar, and A. Professor, "Characterization of GFRP Material," 2021.

[5] S. Dhipanaravind and R. Sivagamasundari, "Flexural Behaviour of Concrete Oneway Slabs Reinforced with Hybrid FRP Bars," 2018. [Online]. Available: http://www.ripublication.com

[6] S. H. Al-Tersawy And M. A. Ghanem, "Ductility And Flexural Behavior Of One Way Concrete Slabs Reinforced With Local Gfrp Rebars: An Experimental And Analytical Study," ERJ. Engineering Research Journal, 37(1), pp.95-106, 2014.

[7] A. S. Debaiky, G. Nkurunziza, B. Benmokrane, and P. Cousin, "Residual Tensile Properties of GFRP Reinforcing Bars after Loading in Severe Environments," *Journal of Composites for Construction*, vol. 10, no. 5, pp. 370–380, Oct. 2006, doi: 10.1061/(asce)1090-0268(2006)10:5(370).

[8] K. Chang and D. Seo, "Behavior of One-Way Concrete Slabs Reinforced with GFRP Bars."

[9] I. Hollý, J. Bilčík, O. Keseli, and N. Gažovičová, "Bond of GFRP reinforcement with concrete," *Key Eng Mater*, vol. 691, pp. 356–365, 2016, doi: 10.4028/www.scientific.net/KEM.691.356.

[10] K. Attia, W. Alnahhal, A. Elrefai, and Y. Rihan, "Flexural behavior of basalt fiber-reinforced concrete slab strips reinforced with BFRP and GFRP bars," *Compos Struct*, vol. 211, pp. 1–12, Mar. 2019, doi: 10.1016/j.compstruct.2018.12.016.

[11] M. Al-Rubaye *et al.*, “Flexural behaviour of concrete slabs reinforced with GFRP bars and hollow composite reinforcing systems,” *Compos Struct*, vol. 236, Mar. 2020, doi: 10.1016/j.compstruct.2019.111836.
[12] M. Abdulkhaliq and A. H. Al-Ahmed, “Behavior of GFRP Reinforced-Concrete Bubbled One-Way Slabs by Encased Composite Steel I-Sections,” *Engineering, Technology and Applied Science Research*, vol. 14, no. 5, pp. 16701–16712, Oct. 2024, doi: 10.48084/etasr.8123.
[13] M. A. Golham and A. H. A. Al-Ahmed, “Strengthening of GFRP Reinforced Concrete Slabs with Openings,” *Journal of Engineering*, vol. 30, no. 01, pp. 157–172, Jan. 2024, doi: 10.31026/j.eng.2024.01.10.
[14] ACI Committee 318, *Building Code Requirements for Structural Concrete (ACI 318-19)*. American Concrete Institute, 2019. doi: 10.14359/51716937.
[15] W. Somboonsong, “Development of ductile hybrid fiber reinforced polymer (D-H-FRP) reinforcement for concrete structures,” Drexel University, Philadelphia, Pennsylvania, United States, 1997. doi: 10.17918/00008501.
[16] M. Abdulmuttalib Issa, A. A. Allawi, and N. Oukaili, “Performance of doubly reinforced concrete beams with GFRP bars,” *J Mech Behav Mater*, vol. 33, no. 1, Jan. 2024, doi: 10.1515/jmbm-2022-0308.
[17] V. J. Worner, “Use of Glass Fibre Reinforced Polymer (GFRP) reinforcing bars for concrete bridge decks,” 2015.
[18] F. Oudah and R. El-Hacha, “A new ductility model of reinforced concrete beams strengthened using Fiber Reinforced Polymer reinforcement,” *Compos B Eng*, vol. 43, no. 8, pp. 3338–3347, Dec. 2012, doi: 10.1016/j.compositesb.2012.01.071.
[19] Zayan HS, Ali ZM, Amer OZ, Mahmoud AS. Enhancing the Capacity of Voided Reinforced GFRP One-Way Slabs Using Tact Bundled Waste Plastic Bottles. Eng. 2026 Apr 26;7(5):196, doi: 10.3390/eng7050196.
[20] Fazaa Rajab, Omar, Ziadoon M. Ali, Akram S. Mahmoud, and Majid S. Mohammed. "Flexural Ductility, Stiffness, and Toughness of New Voided Reinforced Concrete One-Way Slab Using Waste Plastic Bottles." Journal of Engineering 2022, no. 1 (2022): 8672694, doi: 10.1155/2022/8672694.
[21] Mohammed, Majid S., Mohammed L. Ahmed, Ziadoon M. Ali, and Akram S. Mahmoud. "An innovative method of voided reinforced concrete one-way slabs using bundled waste PET bottled tubes." In Materials Science Forum, vol. 1007, pp. 76-84. Trans Tech Publications Ltd, 2020, doi:10.4028/www.scientific.net/MSF.1007.76
[22] M. R. Rasheed and S. D. Mohammed, “Structural behavior of one-way slabs reinforced by a combination of GFRP and steel bars: An experimental and numerical investigation,” *J Mech Behav Mater*, vol. 33, no. 1, Jan. 2024, doi: 10.1515/jmbm-2024-0002.